International Journal of Pharmaceutics 391 (2010) 98–106

Contents lists available at ScienceDirect

International Journal of Pharmaceutics

journal homepage: www.elsevier.com/locate/ijpharm

An assessment of beclomethasone dipropionate clathrate formation in a model suspension metered dose inhaler

Abdennour Bouhroum[a], Jonathan C. Burley[a], Neil R. Champness[b], Richard C. Toon[c], Philip A. Jinks[c], Philip M. Williams[a], Clive J. Roberts[a,*]

[a] Laboratory of Biophysics and Surface Analysis, School of Pharmacy, University of Nottingham, University Park, Nottingham, NG7 2RD, UK
[b] School of Chemistry, University of Nottingham, University Park, NG7 2RD, UK
[c] 3M Drug Delivery Systems, 1 Morley Street, Loughborough, Leicester, LE11 1EP, UK

ARTICLE INFO

Article history:
Received 21 December 2009
Received in revised form 9 February 2010
Accepted 11 February 2010
Available online 23 February 2010

Keywords:
Clathrate
Pressurised metered dose inhalers (pMDIs)
Atomic force microscopy (AFM)
Surface energy (SE)
Force of adhesion (F_{adh})

ABSTRACT

The aims of this study were to investigate and characterize the physico-chemical properties of beclomethasone dipropionate (BDP) crystallized from tricholoromonofluoromethane (CFC-11). Physical interactions in a model pressurised metered dose inhaler (pMDI) system and changes in surface energy after size reduction (micronization) were determined. Although CFC-11 has largely been phased out of use in pMDIs due to its ozone depletion potential, the BDP CFC-11 clathrate is a stable entity and thus suitable as a model for our initial investigations. In addition, although propellant clathrates have been known for sometime, as far as the authors are aware, their surface energies and adhesive interactions have not been reported. The structure of the clathrate was investigated using scanning electron microscopy (SEM), X-ray photoelectron spectroscopy (XPS) and X-ray powder diffraction (X-RPD). In addition, atomic force microscopy (AFM) was employed to determine the dispersive surface free energy (SE) and force of adhesion (F_{adh}) of the BDP CFC-11 clathrate with different pMDI components in a model propellant (decafluoropentane).

The dispersive surface free energies for anhydrous BDP (micronized), the CFC-11 clathrate and ball-milled BDP CFC-11 clathrate are $(47.5 \pm 4.9)\,mJ\,m^{-2}$, $(11.3 \pm 4.1)\,mJ\,m^{-2}$ and $(15.2 \pm 1.3)\,mJ\,m^{-2}$ respectively. Force of adhesion results shows that BDP CFC-11 clathrates, even after being ball-milled for 2.5 h, have a lower F_{adh} compared to micronized anhydrous BDP with different pMDI components. This shows that the formation of the crystalline CFC-11 clathrate is advantageous when compared to the micronized anhydrous form, in terms of its surface energy and potential interactions within a suspension MDI formulation. In the wider context, this work has implications for the future development of HFA formulations with APIs which are prone to the formation of propellant clathrates.

1. Introduction

The replacement of chlorofluorocarbon (CFC) with hydrofluoroalkane (HFA) propellants has challenged formulators of pressurised metered dose inhalers (pMDIs) in several major aspects. Due to the increased polarity of HFA, the use of alternative (soluble) surfactants or co-solvents, along with traditional surfactants, is required in order to stabilize pressurised suspension products. The surfactant type and composition, as well as drug concentration and particle size, may have an effect on the solubility of an active pharmaceutical ingredient (API), and any related crystal growth could affect the efficacy of a formulation (Smyth, 2003).

Clathrates are a class of inclusion compounds, which generally consist of two molecular species. These arrange themselves in space, so that one molecule (host) entraps the other (guest) (Englezos, 1993) in polyhedral cavities (Koh, 2002). Guest molecules can fully occupy (bonded to the host network) or partially occupy (occupying void spaces) the cages in the host framework (Patchkovskii and Tse, 2003). The thermodynamic stability of the clathrate depends strongly on the size and shape of the guest molecules which must be small enough to fit into the cavities of the lattice, but large enough to lend stability to the structure (Buffett, 2000).

Spontaneous crystal growth occurs rapidly when anhydrous BDP is dispersed in CFC-11 with the formation of the BDP CFC-11 clathrate. The structure is stabilized through hydrogen bonding. Since solid state chemistry can significantly alter the physical interactions within a suspension formulation, it is important to determine the most stable crystalline forms of BDP in the presence of the propellant.

The aims of this study were to investigate and characterize the physico-chemical properties of beclomethasone dipropionate

* Corresponding author. Tel.: +44 115 9515048; fax: +44 115 8467969.
E-mail address: clive.roberts@nottingham.ac.uk (C.J. Roberts).

0378-5173/$ – see front matter © 2010 Elsevier B.V. All rights reserved.
doi:10.1016/j.ijpharm.2010.02.024

(BDP) crystallized from tricholoromonofluoromethane (CFC-11). Physical interactions in a model pressurised metered dose inhaler (pMDI) system and the effect of size reduction (ball-milling) on surface energy was also determined.

2. Materials and methods

2.1. Materials and sample preparation

Anhydrous BDP (micronized) was purchased from Sicor (UK); 1,1,2-tetrafluoroethane (HFA 134a) was supplied by Dupont (UK) and CFC-11 was supplied by Arkerma (UK). All other chemicals were purchased from Sigma–Aldrich Company Ltd. (UK), unless otherwise indicated. 3 M Drug Delivery Systems (UK) supplied a micronized isopropyl alcohol (IPA) clathrate of BDP for investigation (EP 205530).

2.1.1. Isolation of stable BDP CFC-11 clathrate

Anhydrous BDP was suspended in CFC-11 in a pressure resistant vial. The concentrations of the drug were, 0.1, 0.5, 1.67, 2, 2.5 and 3% (w/w) BDP in CFC-11. All formulations were shaken using a Stuart SF1 flask shaker for 2 h at 800 oscillations-per-minute and stored at 5 °C for 24 h. The material was isolated by vacuum filtration using a glass filter, washed three times, using the filtrate suspension, in order to filter as much as possible of the suspension. Excess propellant was then removed by evaporation for 24 h under room temperature and pressure (Phillips and Byron, 1994).

2.1.2. Isolation of BDP ethanol (EtOH) HFA-134a clathrate and BDP EtOH solvate

Attempts to obtain BDP EtOH HFA-134a crystals from a suspension of anhydrous BDP in 20% (w/w) absolute ethanol and HFA-134a in a pressure resistant vial were undertaken (Harris et al., 2003). The suspension was cooled down to below the HFA-134a boiling point −26.5 °C, using a cooling bath, containing dry ice and acetone. The crystals were isolated by vacuum filtration of the solution using a glass filter. Excess propellant was removed by evaporation at ambient temperature and pressure for 24 h (Harris et al., 2003).

BDP EtOH solvate crystals were grown in a 3% (w/w) supersaturated solution of EtOH at 70 °C (Harris et al., 2003). The solution was then allowed to equilibrate for 3 h at room temperature before being at 5 °C for 24 h. The extraction of crystals was done via rotary evaporation (Kuehl et al., 2003).

All the prepared crystals were placed in a dry container (container dried in an oven for a few hours before use). The headspace of the container was flushed with nitrogen before the closure of the container and sealed. The operation was repeated each time the container was opened. All containers were placed in a desiccator in order to ensure the integrity of the crystal during storage. The different preparations were made in triplicate and all samples were analysed, in triplicate, using the different characterization techniques described.

2.1.3. Clathrate size reduction (ball-milling)

Size reduction on the BDP CFC-11 clathrate was carried out by ball milling using a Restsch® MM 400 ball-miller (Restsch, Germany). The milling intensity was the maximum with a frequency of 30 Hz and was carried out for 2 h on 500 mg of the BDP CFC-11. The size and morphology of the ball-milled particles were studied by SEM. The samples were used for surface energy determination and force of adhesion with different pMDI components. The samples were sealed under nitrogen and stored at 5 °C.

2.2. Characterization techniques

2.2.1. Scanning electron microscopy (SEM)

The particle size and morphology were analysed by SEM using a JEOL JSM-6060LV (JEOL (UK) Ltd., Welwyn Garden City, UK) at various magnifications. The samples prepared as above, were mounted onto carbon stubs and then sputter coated with a thin layer of gold in an argon atmosphere (50 Pa) at 30 mA for 4 min for SEM analysis. For BDP CFC-11 clathrates, SEM images were taken before and after heating the samples to 150 °C in order to determine whether any morphological changes occur after the release of the propellant.

2.2.2. X-ray powder diffraction (X-RPD)

X-RPD patterns were collected on a Bruker D8 diffractometer system (Bruker AXS, Madison, WI, USA), operating in a Debye-Scherrer geometry. A ceramic X-ray tube with a copper target, wavelength (λ) 1.54059 Å, operated at 40 kV, 40 mA. A scintillation counter was employed. The X-ray patterns were analysed using the Le Bail method to model the patterns obtained, based on the reported unit cell for the clathrate. The patterns obtained for the crystals were obtained before and after heating the different samples. All the patterns were collected straight after the formation of the crystals and after heating them to 150 °C in order to determine if there are any structural changes after the removal of the propellant. For the BDP EtOH HFA-134a clathrate, the patterns collected were after heating the samples to 100 °C and then to 150 °C, due to the presence of two different peaks on the DSC trace.

2.2.3. X-ray photoelectric spectroscopy (XPS)

BDP and BDP CFC-11 clathrate samples were analysed using XPS in order to determine surface elemental composition using a Kratos AXIS ULTRA spectrometer (Kratos Analytical, Manchester, UK) with a mono-chromatic Al Kα X-ray source (1486.6 eV) operated at 15 mA emission current and 10 kV anode potential. The ULTRA was used in fixed analysed transmission (FAT) mode, with pass energy of energy 20 eV for high resolution scans. A wide survey scan and high resolution scans were performed on each sample. Wide scans were run for 5–10 min and high resolution scans for 10–30 min. Data analysis was carried out using CASAXPS software with Kratos sensitivity factors to determine the atomic percentage values from the peak areas. The irradiating X-rays were emitted at a take-off angle of 90°.

2.2.4. Thermogravimetric analysis (TGA)

A SDT Q600 TGA/DSC was used to record the weight loss of the samples between 0 °C and 300 °C. Dry nitrogen gas was used as a purge and the scan speed was 10 °C min^{-1}. An isothermal period at 25 °C was run for 10 min prior to the measurements and any changes in weight during that period were monitored. In all measurements between 6 mg and 7 mg of sample was used. The thermograms obtained from the TGA results were analysed using TA universal analysis -NT software.

2.2.5. Differential scanning calorimetry (DSC)

DSC experiments were carried out using a DSC 2920 Differential Scanning Calorimeter (TA Instruments, USA), with a constant 10 °C min^{-1} heating rate, from 0 °C to 300 °C in a dry nitrogen atmosphere. Non-sealed aluminium pans were used in order to allow the escape of the propellant during the desolvation phase. In all measurements between 6 mg and 7 mg of sample was used. When required, simultaneous TGA/DSC measurements were performed under identical conditions using a SDT Q600 TGA/DSC (TA Instruments, USA). The thermograms obtained for the DSC results were analysed using TA universal analysis -NT software.

2.2.6. Surface energy measurements

The surface energy of each material was determined using the blank AFM cantilever method (Davies et al., 2005) where three Force Modulation Etched Silicon Probes (FESP) cantilevers (Veeco, Santa Barbara, CA, USA) were used to determine the F_{adh} from compacts of each clathrate and anhydrous BDP (Stegemann et al., 2007). In order to find out the flexibility (and hence exerted force) of each cantilever, the spring constants of these FESP cantilevers were determined using the Sader method prior to force data acquisition (Sader et al., 1995). The spring constants for the FESP tips were between 2.8 N m^{-1} and 3.6 N m^{-1}. The surface energies of the API materials were then determined based on the known surface energy of the silica probe and the measured adhesion to each API. Before force acquisition, each cantilever probe was cleaned using a UV cleaner (Bioforce Nanosciences, Ames, IA, USA) for 20 min to remove organic contaminants on the probe surface. The force of adhesion (F_{adh}) measurements were then determined using an EnviroScope AFM (Veeco). The tests were conducted at ambient temperature (20 °C) and relative humidity (RH) of less than 1%. A Triton Laboratory Instrument Control Application, version 1.0.32 (Triton Technology, Keyworth, UK) controlled and maintained the humidity within the chamber.

One hundred force measurements were recorded using each cantilever, employing a distance of 100 nm between sampling points. Force curves using each cantilever were also immediately collected against a freshly cleaned borosilicate glass cover-slip, before and after the F_{adh} measurements. The borosilicate cover slip was used as a non-indenting reference to determine the sample deformation. The cover slip was cleaned, rinsed and dried using Piranha solution [a mixture of 30% H_2O_2 and 70% concentrated H_2SO_4 in water (1:4)], deionised water and nitrogen gas respectively. Before and directly after all force measurements, the tip radius of each single probe used was characterized by tip self-imaging in order to check the integrity of the tip throughout the experiment (Davies et al., 2005). Following AFM measurements, the functionalised V-shaped cantilevers were analysed using SEM again to ensure that the imaging and force measurements had not changed the particle morphology or removed the particles completely from the apex of the AFM cantilever.

2.2.7. Topographical imaging of the different clathrates

Each material was topographically imaged using a Nanoscope IIIa MultiMode AFM (Veeco) in contact mode using NPS cantilevers (Veeco). A scan rate of 0.5 Hz was used over a 0.5 μm × 0.5 μm scan size. This was done to determine the root mean square (RMS) roughness of each API using the topographical software incorporated within the AFM system.

2.2.8. AFM adhesion measurements

AFM was used in order to measure the interactive forces between the anhydrous BDP, BDP CFC-11 clathrate, BDP IPA clathrate, ball-milled BDP CFC-11 clathrate and chosen components. This was performed using the colloid probe technique, where particles of each API material were attached to AFM cantilevers (Davies et al., 2005). To summarize, single particles of each API were attached to individual cantilevers using an epoxy resin. The spring constants for each cantilever (determined using the thermal method (Gibson et al., 2003)) ranged between 0.3 N m^{-1} and 0.5 N m^{-1}. Correct positioning of the particle on the cantilever was verified using SEM before and after AFM analysis (note: the samples were not gold coated, as this would clearly render the tips unsuitable for use). Three probes were prepared for each API. Prior to force measurement analysis, each probe was imaged using a tip-characterisation method described elsewhere (Hooton et al., 2002). Imaging and force determination were performed using an EnviroScope AFM. One hundred force measurements were taken using each probe against the surfaces of anhydrous BDP, BDP CFC-11 clathrate, and BDP IPA clathrate in the presence of 20 ml of a model propellant 2H, 3H decafluoropentane (mHFA) (Sigma–Aldrich, UK). The measurements were conducted at 10 °C and at a RH of 25%. The force data were integrated and calculated using custom software. The separation energy between each API and each pMDI surface was determined by integrating the area under each force curve produced, using in-house software.

F_{adh} between each probe and the substrate was determined using AFM. From these results, the Work of Adhesion (W_A) was calculated using the equation:

$$W_A = \frac{3F_{adh}}{2\pi R} \quad (1)$$

where, R is equal to the radius of the hemispherical point of contact (assumed in accordance with the Johnson–Kendall–Roberts theory) determined by tip characterisation. The surface free energy of each material was calculated as described previously (Davies et al., 2005).

3. Results and discussion

3.1. Morphological comparison between BDP CFC-11 clathrates and BDP EtOH HFA-134a clathrates

The BDP CFC-11 clathrates showed a rapid growth of the crystals. SEM images of the particles are shown in Fig. 1A. The micrographs obtained with BDP CFC-11 indicate the formation of well-defined crystals with hexagonal morphology. The crystals are poly-dispersed, with a size range of 30–70 μm.

An SEM image of crystals obtained from BDP in HFA-134 and ethanol is shown in Fig. 1B. Crystalline particles smaller than the BDP CFC-11 clathrate are observed. The particles are mostly aggregated into small clusters and do not show significant polydispersion. The crystal particle size could not be readily identified due to aggregation. The crystals seem to have a particle size of less than 5 μm. However, the isolation and characterisation of the HFA-134, ethanol clathrate of BDP remains challenging.

3.1.1. X-ray powder diffractometry (X-RPD)

Diffraction techniques are definitive tools for detecting and quantifying molecular order in a system (Shah et al., 2006). Four crystal structures have been reported and filed with the Cambridge Structural Database (CSD) for BDP and its compounds: one for anhydrous BDP (Millard and Myrdal, 2002); one for BDP monohydrate (Duax et al., 1981); one for the HFA-134a clathrate (Harris et al., 2003); and one for the BDP ethanol clathrate (Kuehl et al., 2003). For the clathrates, only partial crystal structures are available: the guest molecules are disordered and only the atomic co-ordinates of the framework BDP molecules have been reported. The two reported clathrate structures are identical for all intents and purposes. The single-crystal derived structural data reported in the literature for these compounds were determined at 100 K, 271 K, 170 K and 170 K respectively.

For the sample of as-received anhydrous BDP, when the effects of thermal expansion are accounted for, we achieve an excellent match when comparing our room temperature data with a pattern calculated from the reported 100 K structure of BDP (ca. fractional increase in volume at room temperature compared to 100 K of 4.5%). The Rietveld method was used to model the entire powder pattern profile and to calculate lattice parameters. The as-received material can therefore be unambiguously identified as identical with the previously reported anhydrous BDP (Millard and Myrdal, 2002), and our bulk sample, which is predominantly crystalline, and pure, within the limits of our data collection, analysis, etc.A reasonable match was obtained for our BDP CFC-11 clathrate when

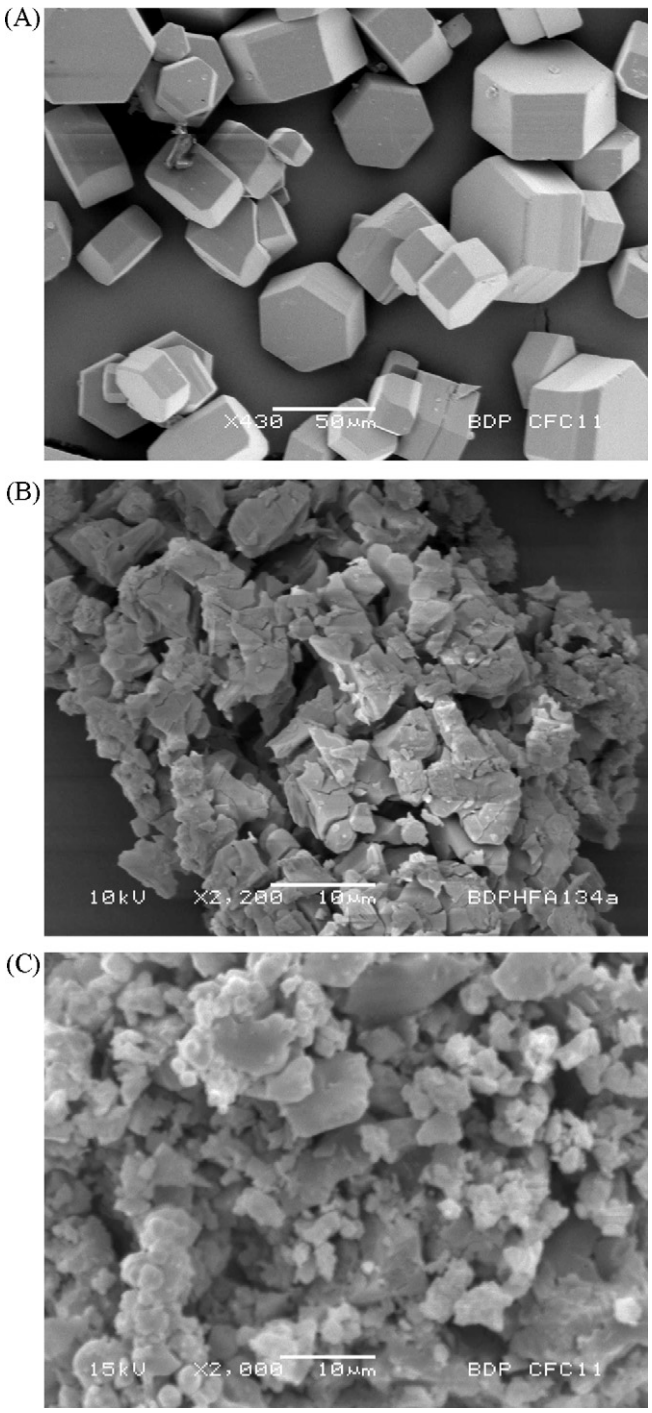

Fig. 1. (A) SEM photographs of BDP CFC-11 clathrate (1.67% (w/w) anhydrous BDP in CFC-11), (B) BDP EtOH HFA-134a clathrate (3% (w/w) anhydrous BDP in HFA-134a) and (C) ball-milled BDP CFC-11 clathrate.

comparing our data with patterns calculated based on the partial structures reported for the BDP HFA-134a and BDP ethanol clathrates (Fig. 2A). The lack of a precise match is expected given that the reported structures do not include the guest molecules. A more rigorous comparison, using the Le Bail method (Le-Bail et al., 1988) to fit the observed pattern using the unit cell reported for the clathrate (and allowing for thermal expansion, ca. fractional increase in volume at room temperature compared to 170 K of 1.5%) produces an excellent fit of the data, with no extra peaks present in the pattern. Particular care was taken to examine the regions of the pattern where peaks from anhydrous BDP might be observed.

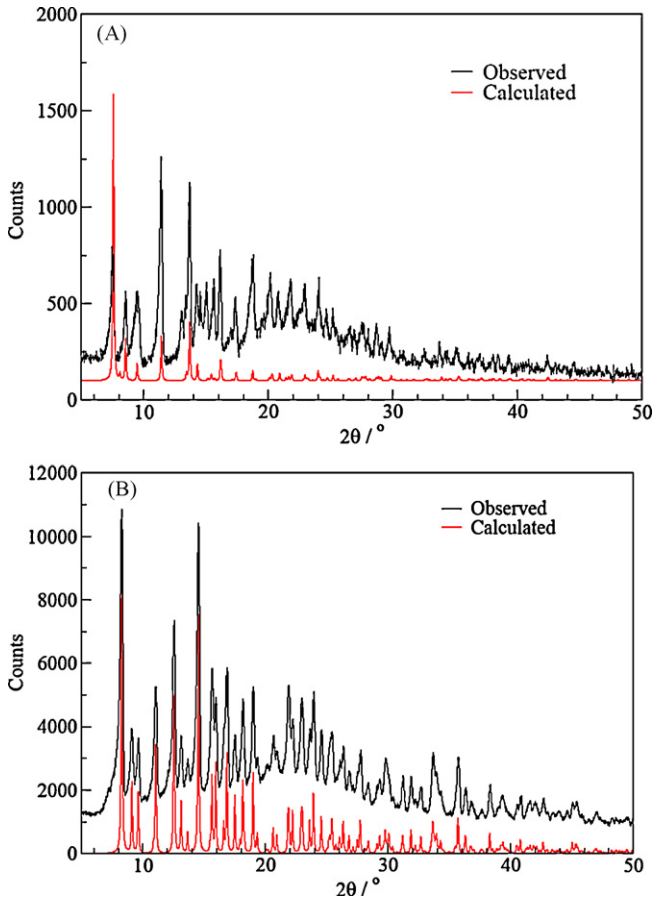

Fig. 2. (A) Superimposition of experimental BDP CFC-11 clathrate X-RPD pattern with that of the calculated BDP EtOH HFA-134a clathrate X-RPD pattern without the solvent. (B) Superimposition of experimental BDP EtOH HFA-134a clathrate X-RPD pattern with that of BDP monohydrate.

In addition to providing confidence that the bulk sample of BDP CFC-11 clathrate is pure (and has the clathrate unit cell), the Le Bail method allows us to estimate the "idealized" composition of the clathrate if space filling is assumed. Using the tabulated atomic volumes of Hofmann (2002) and Himes and Mighell (1987), a single BDP molecule is expected to occupy ca. 685 Å^3. Given that at room temperature the unit cell volume is 4959 Å^3 from our Le Bail analysis, and that the unit cell of the clathrate contains six BDP molecules (Harris et al., 2003; Kuehl et al., 2003), there is 850 Å^3 of void space. If this void space is completely occupied by CFC-11 of approximate volume 100 Å^3 per molecule, the overall stoichiometry for the CFC-11 clathrate is expected to be approximately BDP CFC-11 1:1.4. Likewise, for an EtOH molecule of approximate volume 70 Å^3, a stoichiometry of BDP EtOH of 1:2 is expected.[1]

The powder pattern of the nominal BDP EtOH HFA-134a clathrate did not match patterns calculated based on the reported clathrate structures, but instead an excellent match was obtained for a pattern calculated from the reported BDP hydrate structure (Duax et al., 1981) (Fig. 2B). We therefore conclude that the mixed BDP EtOH HFA-134a clathrate converts rapidly to the hydrate in the presence of water (Harris et al., 2003).

The powder pattern of BDP CFC-11 clathrate, collected after heating the sample to 150 °C at standard atmospheric conditions,

[1] These stoichiometries are necessarily estimates. For comparison, the unit cell volume of anhydrous BDP is 2655.9 Å^3 from X-RPD, and 2680 Å^3 from the simple atomic volume calculation, which corresponds to a volume-per-BDP molecule of 664 Å^3 from X-RPD vs 670 Å^3 from the simple calculation.

Table 1
Theoretical and measured atomic percentage of the surface analysis of anhydrous BDP, BDP CFC-11 (0.5% (w/w)) and BDP IPA clathrate.

Atomic %	Anhydrous BDP		BDP CFC-11 clathrate		BDP IPA clathrate	
	Theoretical	Measured	Theoretical	Measured	Theoretical	Measured
C 1s	77.77	81.07	68.37	75.1	77.5	81.34
O 1s	19.44	17.01	16.28	18.54	20	16.54
Cl 2p	2.78	1.914	12.09	5.43	2.5	2.23
F 1s	0	0	3.25	0.92	0	0

was distinctly different to patterns calculated based on all previously reported structure, and also different to all patterns that we have collected in this study. The new pattern was characterised by strong diffraction peaks, and represents a new polymorph of BDP. A separate communication will report on this and on a detailed study of the transformation itself.

3.2. BDP and BDP CFC-11 clathrate surface chemical analysis

Both anhydrous BDP and BDP CFC-11 clathrate were analysed using XPS and ATR-IR spectroscopy in order to determine the elemental composition of each of the compounds in particular CFC-11 inclusion.

ATR-IR spectroscopy was performed on a small amount of the different concentrations of BDP CFC-11 clathrates (results not shown) in order to show the presence of fluorine on the clathrate crystal obtained. The spectra obtained showed a very noticeable peak at a wavenumber of around 1000 cm^{-1}. This peak was ascribed to CFC-11 peak [Integrated Spectral Database System of Organic Compounds (SBDS)].

The surface composition of both BDP CFC-11 clathrate at a concentration of 0.1% (w/w) and 0.5% (w/w) BDP in CFC-11 did not show any significant changes in the atomic percentage of all the atoms present in the structure between the two different concentrations (Table 1). A very small change on the atomic percentage can be noticed for both anhydrous BDP and BDP IPA clathrate. The changes are more noticeable with high resolution scans (results not shown) which show a slight difference in the number of the carbonyl groups. The results obtained for both anhydrous BDP and BDP IPA clathrate (ratio of 1:1.5 BDP to IPA as IPA has about 94 $Å^3$) are quite consistent and comparable to the theoretical atomic percentage calculated (Table 1). However, for BDP CFC-11 clathrate, the results obtained seem quite different from the theoretical atomic percentage calculated for the 1:1.4 molar ratio of BDP to CFC-11. The results obtained showed a 1:0.4 molar ratio of BDP to CFC-11 for the two concentrations stated above. In order to confirm the molar ratio observed by XPS, a quantitative elemental analysis on the BDP CFC-11 clathrate of 0.1% (w/w) and 0.5% (w/w) BDP in CFC-11 was performed. The analysis was accomplished via the combustion of the crystal and the collection of combustion product which is weighed and used in order to calculate the composition of the unknown samples. The results showed an average of 58.90% carbon and 6.48% hydrogen.

To summarize, X-RPD, XPS and ATR-IR results show that the successful formation of pure, although sub-stoichiometric BDP CFC-11 clathrate was determined.

3.3. Thermal analysis

3.3.1. Thermogravimetric analysis (TGA)

TGA relies on a high degree of precision in three measurements: weight, temperature, and temperature change (Shah et al., 2006). No weight loss was observed for anhydrous BDP between 0 °C and 212 °C (results not shown). The loss of CFC-11 from the clathrate structure, observed at around 100 °C is confirmed by the TGA results and was observed with the different BDP CFC-11 clathrates over the range of concentrations used for the study (results not shown). The loss of CFC-11 is expressed by a weight loss of 14.5% which corresponds to a 1:0.6 molar ratio of CFC-11 to BDP for a BDP CFC-11 clathrate (1.67% (w/w) anhydrous BDP suspended in CFC-11). Different samples of clathrates formed by using different concentrations of BDP in CFC-11 showed a different weight loss (Table 2). The percentage weight loss for this latter material also differs from the theoretical weight loss calculated for a molar ratio of 1.4:1 CFC-11 to BDP. All the measured weight losses of CFC-11 from the clathrates were lower than expected. It was found from these results that CFC-11 was successfully included in the crystal structure for the different concentrations to form a clathrate. The TGA data for the BDP:EtOH solvate showed weight loss as soon as the samples were placed in the instrument, before and as soon as heating was applied (results not shown). This loss of EtOH from the structure as soon as the heating was initiated is consistent with the results observed using DSC. Furthermore, the measured weight loss was similar to the theoretical weight of BDP:EtOH solvate at a 2:1 molar of EtOH in BDP confirming the formation of a solvate. BDP:IPA clathrate TGA results show similar results to BDP EtOH solvate without the initial weight loss observed at the beginning of heating (results not shown).

Clathrates are described as crystalline solids in which guest molecules occupy cavities or channels in the host lattice that are formed upon crystallization (Vaidya, 2004). However, in non-clathrate crystal formations, i.e. solvates, the individual molecules are tightly packed together, with intermolecular spaces between neighbouring entities filled by a second, solvent-type molecule or used to complete a coordination sphere around a functional moiety (Vaidya, 2004). The solvent entities are rather loosely held in the lattice. The stoichiometric relationship between host and solvent are quite difficult to predict as it depends on the size of the voids and the actual size of the solvent and how these interact (Goldberg, 1988). Many of the solvates can therefore be considered as a special type of clathrate structure.

Stoichiometric analysis of the clathrates studied in this work shows a ratio of host to guest molecules slightly lower than would be expected. This indicates that all of the available cavities are not filled. This can be explained by considering the process of clathrate formation where it is thought that clusters of host molecules begin to form in solution surrounding the guest molecules, when the agglomeration of host molecules reaches a critical size crystal growth begins. If the guest molecule is not correctly positioned or oriented at this point it will not be enclosed and thus some empty cavities are to be expected (Kuhs et al., 1997, Vaidya, 2004). In addi-

Table 2
The different crystal samples encountered together with experimental (TGA) and calculated weight loss in weight %.

Samples	Weight loss TGA/% (w/w)	Theoretical weight loss %
BDP CFC-11 clathrate 1.67% (w/w)	13.8	19.72 (1:1.4 BDP to CFC-11)
BDP EtOH solvate	9.7	8.19 (1:1 BDP to EtOH)
BDP monohydrate	–	3.39 (1:1 BDP to H_2O)
BDP IPA clathrate	10.5	18.7 (1:2 BDP to IPA)

Table 3
Stoichiometric relationship of BDP CFC-11 clathrate using calculation of molar ratio of CFC-11 to BDP using results obtained from TGA.

BDP CFC-11 clathrate concentration % (w/w)	0.1	0.5	1.67	2	2.5	3
Number of CFC-11 molecules trapped in the channels	0.1 ± 0.02	0.4 ± 0.04	0.6 ± 0.037	0.35 ± 0.05	0.4 ± 0.02	0.15 ± 0.03

tion the level of cage occupation is thought to be influenced by the pressure and temperature at formation. It is also possible for each channel to contain multiple small guest molecules (Kuhs et al., 1997).

The TGA results were used to determine the number of CFC-11 molecules present in the channels of the clathrate structure and the EtOH molecules in the solvate structure. The results for the BDP:EtOH solvate showed a 1:1 molar ratio of BDP to EtOH. In contrast, the TGA data collected for the different concentrations of BDP CFC-11 clathrates showed a different molecular ratio of CFC-11 to BDP with different concentrations of BDP CFC-11 clathrate (Table 3). The stoichiometric relationship is hence not clear but appears to show an increased molar ratio of CFC-11 to BDP with increasing concentration of BDP to CFC-11 during the conversion. At 1.67% (w/w) of BDP to CFC-11, it reaches its maximum with a 0.6:1 molar ratio of CFC-11 to BDP and then decreases as the concentration increases (Table 3). The content of CFC-11 in ball-milled BDP CFC-11 clathrate was also determined using TGA and showed no variation in the number of CFC-11 molecules entrapped in the BDP channels (results not shown).

The TGA results obtained for BDP EtOH HFA-134a show a fractional weight loss of 3.3% due to heating from the structure of the clathrate. This represents less than 25% of the theoretical weight loss expected for this compound. After analysis of the data received and the protocol used in order to prepare the BDP EtOH HFA-34a, it can be considered that the crystals analysed may not have been the clathrate but can be attributed to BDP monohydrate. This hypothesis is consistent with the theoretical weight loss expected for BDP monohydrate of approximately 3.4% and confirmed by the X-RPD (Fig. 2B). However, the clathrate might have been synthesized initially as precautions were taken to exclude water contamination. BDP EtOH HFA-134a clathrates are very unstable outside the mother liquor (Harris et al., 2003) and they readily convert to the monohydrate. As the condition for the synthesis of BDP EtOH HFA-134a clathrate require an extremely cold environment of around −50 °C, the clathrates may decompose and convert to the monohydrate form of the steroid once warmed up to room temperature. The decomposition might be seen in the SEM images (Fig. 1B), where small cracks can be observed on the surface of the crystals observed which could be attributed to the release of the EtOH and HFA-134a from the structure prior to imaging. TGA results for BDP EtOH HFA-134a clathrate (Table 2) show the formation of the BDP monohydrate instead of the clathrate as the percentage weight loss obtained for this latter was approximately the same as the theoretical weight loss for the BDP monohydrate.

3.3.2. DSC

DSC is widely used for investigating the phase behaviour of pharmaceutical solids and different methodologies based on instrument type can be utilized (Shah et al., 2006). Conventional DSC, as used here, is based on a linear heating rate of the sample through to its melting point (Shah et al., 2006).

Anhydrous BDP melts at about 212 °C (results not shown) which corresponds to the literature value (Vervaet and Byron, 1999). A thermogram for the BDP CFC-11 clathrate is illustrated in Fig. 3. A small exothermic onset is observed at about 99 °C, which may be due to a solid state rearrangement of the BDP CFC-11 clathrate structure. In addition, an endothermic transition is also seen at about 100 °C and can be slightly variable. This is thought to be due to the release of CFC-11 from the tunnels of the clathrate structure. The melting point of BDP CFC-11 clathrate after CFC-11 loss is seen at approximately 212 °C. The two different transitions for the release of the propellant from the structure are concomitant and cannot be dissociated. The complex thermal events around the melting point observed in the different DSC curves of the different samples indicate that the BDP undergoes significant degradation during melting (Shah et al., 2006). Interestingly, the clathrate retains the solvent (CFC-11) until quite high temperatures are reached (100–120 °C). DSC thermograms were run in cycles in order to check if the transitions were still present after heating. The cycle consisted of heating the samples from 0 °C to 150 °C and then recooling to 0 °C and reheating again to 300 °C. For all the samples

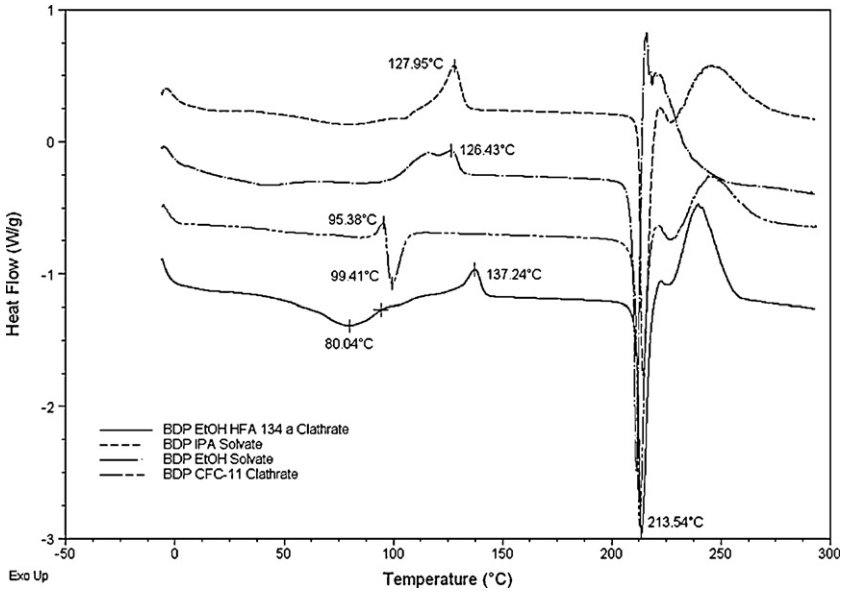

Fig. 3. DSC curves of BDP CFC-11 clathrate, BDP EtOH solvate, BDP IPA clathrate and BDP EtOH HFA 134a clathrate. All samples were heated from 0 °C to 300 °C.

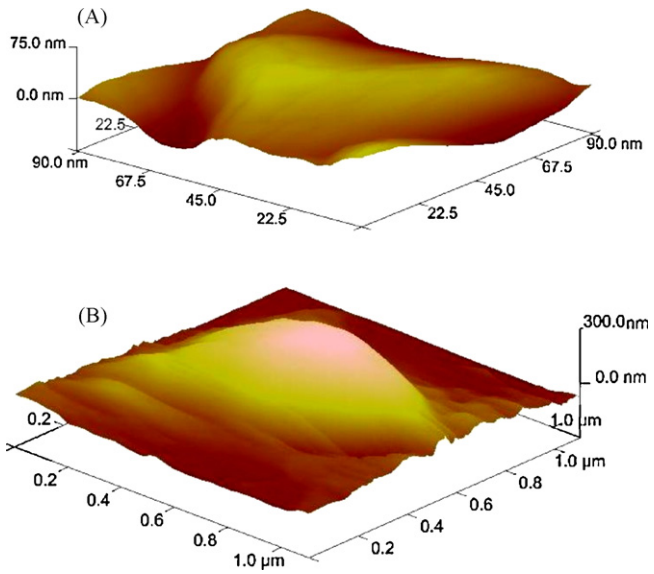

Fig. 4. AFM images of (A) a blank FESP tip image and (B) a particle functionalised tip image.

studied here, the thermograms showed no transitions after initial heating to 150 °C. Therefore, the solid state rearrangement of the clathrate is irreversible and leads to the total loss of the solvent encaged in the channels.

The thermograms for both the BDP:EtOH solvate and BDP:IPA clathrate, showed an exothermic onset at about 110–135 °C and 115–145 °C respectively (Fig. 3). The magnitude of the exothermic transition was slightly variable, due to the non-stoichiometric association of the drug with the solvent (Vervaet and Byron, 1999; Kuehl et al., 2003). The exothermic onsets can be explained by a solid state rearrangement of the structure of the clathrate. A very broad endothermic peak is observed at about 60 °C which is variable between the different batches synthesized and is attributable to the excess EtOH on the samples or on the surface of BDP EtOH solvate.

BDP EtOH HFA-134a thermograms showed a similar pattern to the BDP EtOH solvate with a sharper endothermic peak at about 80 °C and an exothermic peak at around 137 °C (Fig. 3). The two transitions can be explained as the dehydration of the compound, i.e. the loss of the water molecules contained within the structure. As the structure of the hydrate is held in place, mainly via hydrogen bonding between the host and guest molecule, any changes in the structure may lead to a subsequent release of the guest molecules.

3.3.3. AFM topographical imaging of the clathrates

Prior to AFM force measurements, the surface roughness of each BDP entity was quantitatively assessed by AFM imaging to aid the acquisition of local force of adhesion data. The topographical images represented in Fig. 4 illustrate the characterization of both blank and particle functionalised AFM tips. These images were produced *via* an artefact of imaging a tip calibration grating consisting of an array of inverted spikes, with smaller dimensions than those of the tips. Therefore, when attempting to topographically image this sharp surface with an AFM tip, an image of the AFM tip itself is produced. These images demonstrate the approximate sphere-shape of the apex of both the blank tip and functionalised tips at the nanometre scale, thus justifying the use of sphere-plane model geometry, as required by the Johnson–Kendall–Roberts method of γ determination. Both the SEM imaging and tip characterisation imaging of the cantilevers functionalised with the different BDP polymorphs, confirmed the integrity of the particles.

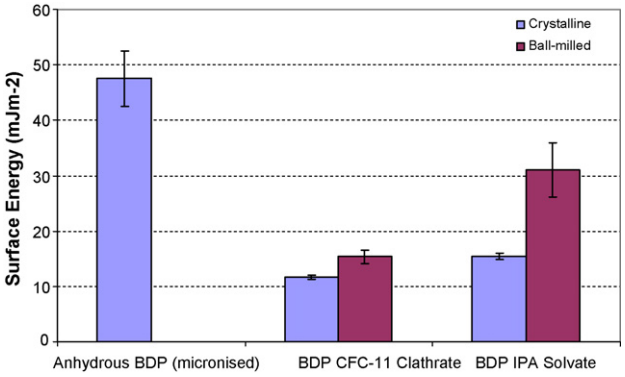

Fig. 5. Surface energy of micronized anhydrous BDP, both crystalline and ball-milled BDP CFC-11 clathrate and BDP IPA clathrate determined by AFM.

The observed mean root mean square (RMS) roughness of each material (3 measurements) is summarized in Table 4. The results show little difference in the RMS roughness for each of these compounds suggesting smooth and ordered surfaces. It is important to characterise the roughness or each BDP entity as surface characteristics of these latter can significantly influence the adhesion with the different pMDI components.

3.3.4. AFM adhesion measurements

A maximum load of 10 nN was applied to push the tips into contact with the sample surfaces. The resultant mean force of adhesion measurements obtained using the colloid probes for each of the materials, are summarized in Table 4. The indentations for each of the materials were recorded and summarised in Table 4. It is clear that there are small differences in the indentation values for the different BDP formulations. This led to differences in the force of adhesion due to changes in contact area as well as material type. Generally, the larger the indentation, the higher the observed F_{adh}.

3.3.5. Surface energy

The γ and W_A values determined using the AFM adhesion data for each BDP formulation using blank FESP tips are summarized in Table 4. The observed ranges of W_A and γ values for each material indicate that the relative surface energies of the BDP formulations rank as follow: micronized BDP:IPA clathrate > micronized anhydrous BDP > ball-milled BDP CFC-11 clathrate > crystalline BDP CFC-11 clathrate. The surface energy of micronized anhydrous BDP, crystalline BDP CFC-11 clathrate, ball-milled BDP CFC-11 clathrate and the micronized BDP:IPA clathrate was determined from AFM force measurements to be $(47.5 \pm 4.9)\,mJ\,m^{-2}$, $(11.3 \pm 4.1)\,mJ\,m^{-2}$, $(15.2 \pm 1.3)\,mJ\,m^{-2}$ and $(66.5 \pm 6.7)\,mJ\,m^{-2}$ (Fig. 5). Tip images obtained using AFM indicate that the structural integrity of each tip was maintained throughout the process of imaging and the force measurements.

The higher surface energy observed for the BDP:IPA clathrate is most likely attributable to its non-solvated nature, since the IPA associated with the BDP IPA clathrate could possibly promote hydrogen bonding. Thus, the surface of the BDP may be more 'active' compared to anhydrous BDP. The higher surface energy of the ball-milled BDP CFC-11 clathrate compared to non-milled BDP CFC-11 clathrate may be due to either the formation of some amorphous material or the exposure of higher energy sites on the surface. This has implications when considering interparticulate interactions, since a higher surface energy typically results in greater cohesive and adhesive properties. The reduction in the dispersive surface energy shows that the formation of the CFC-11 clathrate has a positive effect in terms of reduced interaction within an MDI formulation.

Table 4
RMS roughness of the different BDP formulations used in this study. The mean force of adhesion, work of adhesion and surface free energy of the different BDP clathrates, determined using blank FESP cantilevers.

	RMS roughness (nm)	Indentation depth (nm)	Mean force of adhesion (F_{adh}) (nN)	Mean work of adhesion (W_A) (mJ m^{-2})	Mean surface energy (γ) (mJ m^{-2})
Anhydrous BDP	117.6 ± 5.8	12.4 ± 2.4	127.2 ± 16.4	67.5 ± 8.7	47.5 ± 4.9
BDP IPA clathrate	29.5 ± 6.5	18.3 ± 1.6	199.1 ± 22.4	105.7 ± 11.9	66.5 ± 6.7
BDP CFC-11 clathrate	12.1 ± 4.4	1.7 ± 0.3	8.6 ± 4.1	44.1 ± 0.8	11.3 ± 4.1
Ball-milled BDP CFC-11 clathrate	94.2 ± 17.6	6.3 ± 2.8	126.3 ± 22.8	50.9 ± 2.1	15.2 ± 1.3

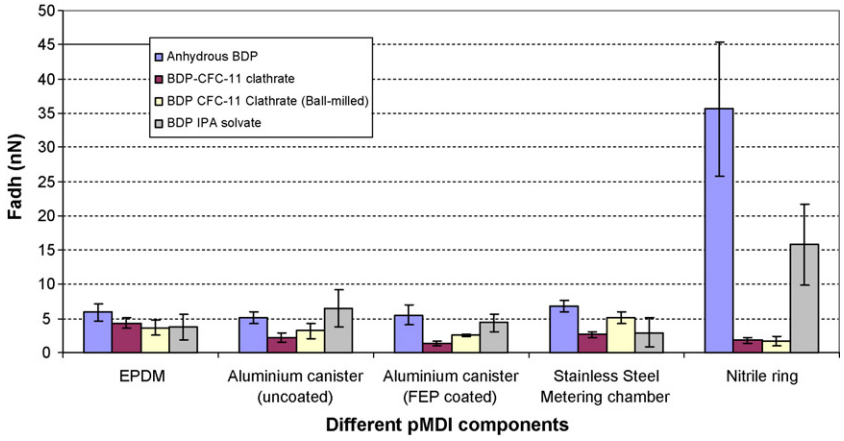

Fig. 6. Force of adhesion of anhydrous BDP, BDP IPA clathrate and BDP CFC-11 clathrate (crystalline and ball-milled) with different pMDI components.

3.3.6. Force of adhesion with different pMDI components

As stated previously, the force of adhesion between each BDP solid form and each pMDI component was determined using AFM (Fig. 6). From this figure, it can be observed that the force of adhesion is highest for the BDP IPA clathrate with the different pMDI components and lowest for the BDP CFC-11 clathrate. Furthermore, ball-milling of the BDP CFC-11 clathrate does not seem to have any major effect in terms of adhesion to the different pMDI components as it showed only a slightly higher F_{adh} than the crystalline BDP CFC-11 clathrate. The F_{adh} for the four different BDP entities with the two types of aluminium canister are approximately the same with a slightly lower adhesion to the fluorinated ethylene propylene (FEP) coated aluminium canister. This is due to the FEP coated aluminium canister having a lower surface energy and a slightly smoother surface than the uncoated aluminium canister. Concerning the F_{adh} of the different BDP entities with the two seals, the results show a very large difference in the adhesive force. Higher F_{adh} values were observed for the different BDP polymorphs with the nitrile ring seal compared to the ethylene diene M-class rubber (EPDM) seal. However, BDP CFC-11 clathrate still showed the lowest adhesion with both seals. The higher F_{adh} seen with the nitrile ring seal could be to the roughness of the surface of the seal and the irregularities of the surface observed using AFM (results not shown).

4. Conclusions

In conclusion, a BDP CFC-11 clathrate has been synthesized and characterized in order to investigate the potential benefits of clathrate formation in metered dose inhaler formulations. The release of CFC-11 from the clathrate form of the steroid was due to a structural rearrangement of the clathrate.

Surface roughness values for each solid form were determined at sample sizes of 5 μm × 5 μm. The different BDP entities ranked in terms of surface roughness as follow: anhydrous BDP > ball-milled BDP IPA clathrate > ball-milled BDP CFC-11 clathrate > BDP IPA clathrate > BDP CFC-11 clathrate.

It was possible to calculate the surface energy of the different materials using single particle adhesion data. The surface free energies for anhydrous BDP (micronized), BDP CFC-11 clathrate (ball-milled for 2.5 h) and the BDP CFC-11 clathrate (crystalline) were (47.5 ± 4.9) mJ m^{-2}, (15.24 ± 1.26) mJ m^{-2} and (11.27 ± 4.05) mJ m^{-2} respectively. Force of adhesion results measured in a model propellant showed that BDP CFC-11 clathrates had a lower F_{adh} compared to anhydrous BDP with the different pMDI components studied and that size reduction of the BDP CFC-11 clathrate did not have any major effect in terms of surface energy and F_{adh}. The adhesive interactions among the three different BDP entities and pMDI components in a model propellant has been characterised using AFM.

The results show that in this case that the *in situ* formation of a clathrate in a propellant formulation is beneficial in terms a reduction the force of adhesion with different pMDI components. This could have implications for future HFA formulation development with APIs that are prone to the formation of propellant clathrates. For example, BDP itself forms a clathrate with HFA 134a over a time scale of months in suspension formulations (Vervaet and Byron, 1999).

References

Buffett, B.A., 2000. Clathrate hydrates. Annu. Rev. Earth Planet. Sci. 28, 477–507.
Davies, M., Brindley, A., Chen, X., Marlow, M., Doughty, S.W., Shrubb, I., Roberts, C.J., 2005. Characterization of drug particle surface energetics and young's modulus by atomic force microscopy and inverse gas chromatography. Pharm. Res. 22, 1158–1166.
Duax, W.L., Cody, V., Strong, P.D., 1981. Structure of the asthma drug beclomethasone dipropionate. Acta Crystallogr. B: Struct. Sci. 37, 383–387.
Englezos, P., 1993. Clathrate hydrates. Ind. Eng. Chem. Res. 32, 1251–1274.
Gibson, C.T., Weeks, B.L., Abell, C., Rayment, T., Myhra, S., 2003. Calibration of AFM cantilever spring constants. Ultramicroscopy 97, 113–118.
Goldberg, I., 1988. The significance of molecular type, shape and complementarity in clathrate inclusion. Topics Curr. Chem. 149, 1–44.
Harris, J.A., Carducci, M.D., Myrdal, P.B., 2003. Beclomethasone dipropionate crystallized from HFA-134a and ethanol. Acta Crystallogr. E 59, 1631–1633.
Himes, V.L., Mighell, A.D., 1987. Nbs crystal data—compound identification and characterization using lattice-matching techniques. J. Metals 39, A29–A129.

Hofmann, D.W.M., 2002. Fast estimation of crystal densities. Acta Crystallogr. B: Struct. Sci. 58, 489–493.
Hooton, J.C., German, C.S., Allen, S., Davies, M.C., Roberts, C.J., Tendler, S.J.B., Williams, P.M., 2002. Characterization of Particle-Interactions by Atomic Force Microscopy: Effect of Contact Area. Pharm. Res. 20, 508–514.
Koh, C.A., 2002. Towards a fundamental understanding of natural gas hydrates. Chem. Soc. Rev. 31, 157–167.
Kuehl, P.J., Garducci, M.D., Myrdal, P.B., 2003. An ethanol solvate of beclomethasone dipropionate. Acta Crystallogr. E 59, 1888–1890.
Kuhs, W.F., Chazallon, B., Radaelli, P.G., Pauer, F., 1997. Cage occupancy and compressibility of deuterated N-2-clathrate hydrate by neutron diffraction. J. Inclus. Phenom. Mol. Recognit. Chem. 29, 65–77.
Le-Bail, A., Duroy, H., Fourquet, A.J.L., 1988. Ab-initio structure determination of $LiSbWO_6$ by X-ray powder diffraction. Mater. Res. Bull., 447–452.
Millard, J.W., Myrdal, P.B., 2002. Anhydrous beclomethasone dipropionate. Acta Crystallogr. E: Struct. Rep. Online 58, O712–O714.
Patchkovskii, S., Tse, J.S., 2003. Thermodynamic stability of hydrogen clathrates. Proc. Natl. Acad. Sci. U.S.A. 100, 14645–14650.
Phillips, E.M., Byron, P.R., 1994. Surfactant promoted crystal growth of micronized methylprednisolone in trichloromonofluoromethane. Int. J. Pharm. 110, 9–19.
Sader, J.E., Larson, I., Mulvaney, P., White, L.R., 1995. Method for the calibration of atomic force microscope cantilevers. Rev. Sci. Instrum. 66, 3789–3798.
Shah, B., Kakumanu, V.K., Bansal, A.K., 2006. Analytical techniques for quantification of amorphous/crystalline phases in pharmaceutical solids. J. Pharm. Sci. 95, 1641–1665.
Smyth, H.D.C., 2003. The influence of formulation variables on the performance of alternative propellant-driven metered dose inhalers. Adv. Drug Deliv. Rev. 55, 807–828.
Stegemann, B., Backhaus, H., Kloss, H., Santner, A.E., 2007. Spherical AFM probes for adhesion force measurements on metal single crystals. Modern Res. Educ. Topics Microsc., 820–827.
Vaidya, S., 2004. Clathrates—an exploration of the chemistry of caged compounds. Resonance 9, 18–31.
Vervaet, C., Byron, P.R., 1999. Drug–surfactant–propellant interactions in HFA-formulations. Int. J. Pharm. 186, 13–30.